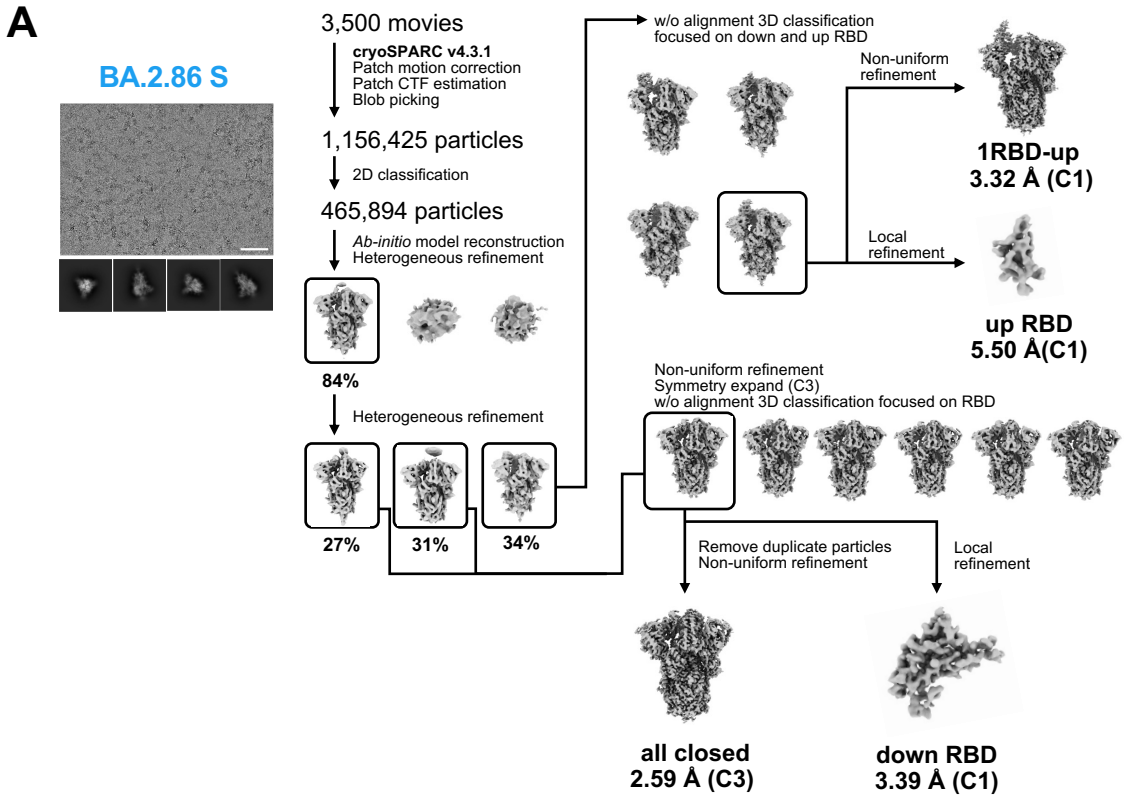

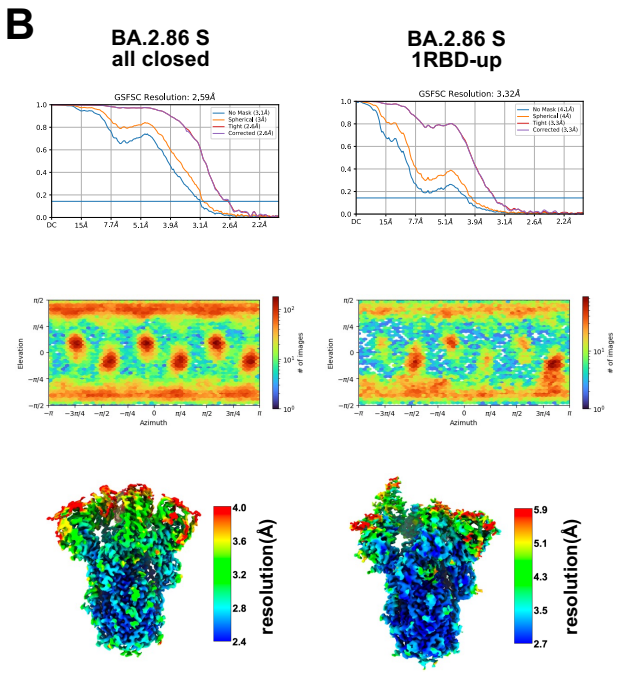

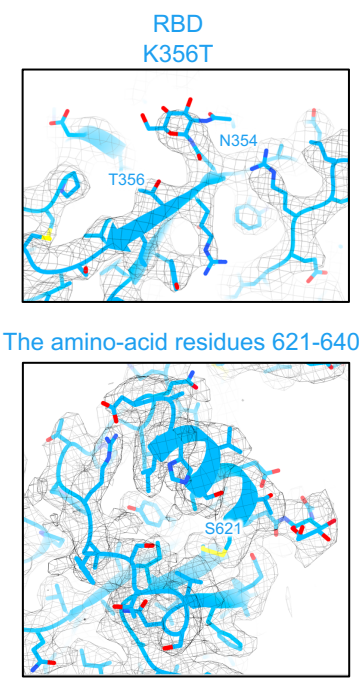

Supplementary Fig. 1. Workflow of cryo-EM data processing for BA.2.86 S and Cryo-EM maps (A) Left: Representative micrograph (scale bars, 50 nm) and 2D class images. **Right:** Cryo-EM data-processing flowchart for BA.2.86 S. **(B) Top:** Global resolution assessment of cryo-EM maps by gold-standard Fourier shell correlation (FSC) curves at the 0.143 criteria. **Middle:** The angular distribution of particles representation by the viewing direction distribution plot. **Bottom:** The calculated values of local resolution are denoted at the grid points of cryo-EM maps. (C) Models fit corresponding cryo-EM maps of residues highlighted in **Fig. 1G**.

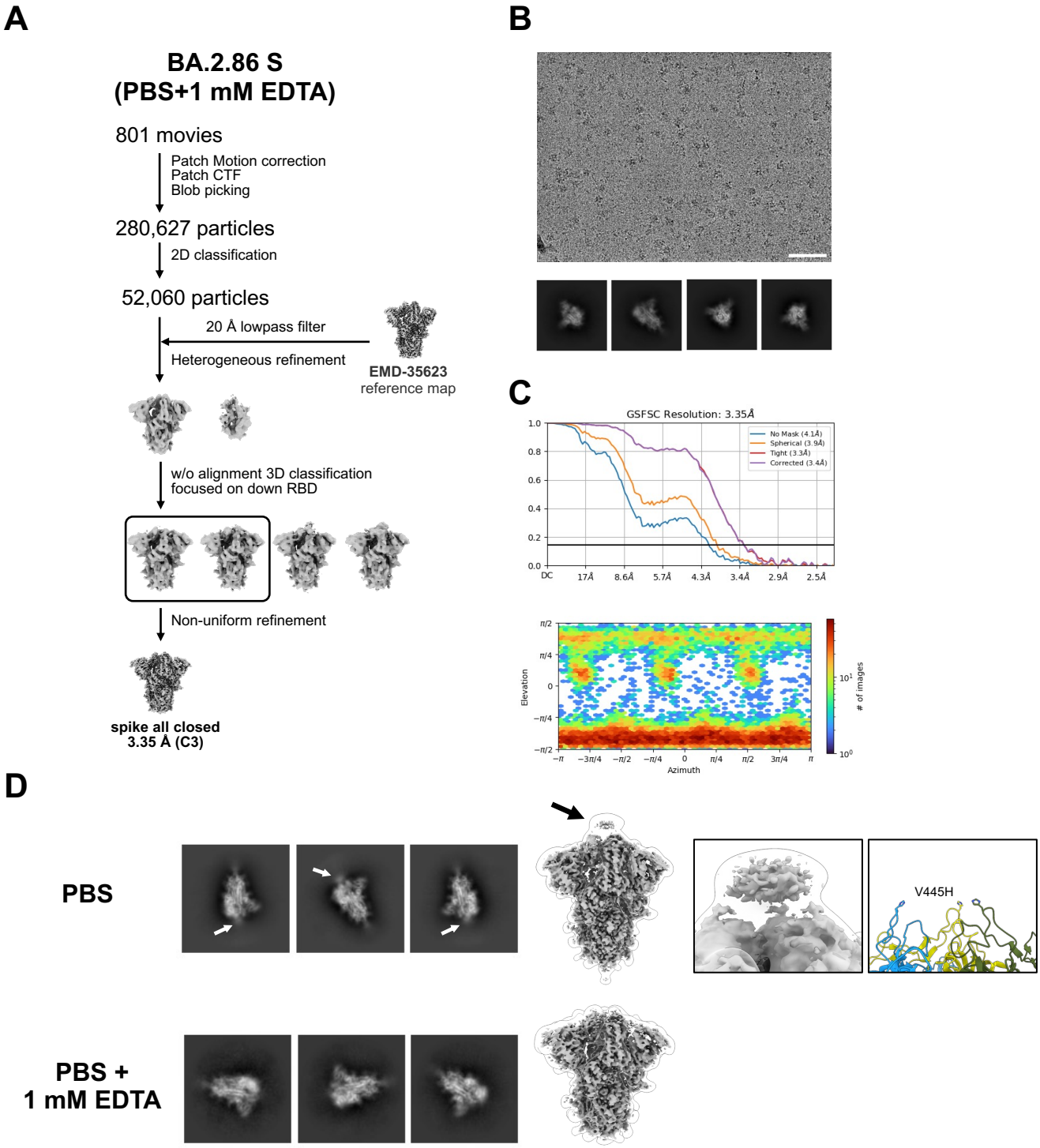

Supplementary Fig. 2. Workflow of cryo-EM data processing for BA.2.86 S-trimer alone with EDTA and comparison of cryo-EM maps with or without EDTA **(A)** Cryo-EM data-processing workflow for SARS-CoV-2 BA.2.86 S in PBS with 1 mM EDTA. **(B) Top:** Representative micrographs (scale bars, 50 nm); **Bottom:** 2D class images. **(C) Top:** Global resolution assessment of cryo-EM maps using gold standard FSC curves at 0.143 criteria. **Bottom:** The angular distribution of particles representation by the viewing direction distribution plot. **(D)** Comparison of single-particle analysis results for BA.2.86 S-protein in PBS and PBS with 1 mM EDTA. **Left:** 2D classification images. **Middle:** Superimposition of 3D cryo-EM maps and 15 Å low-pass filtered maps. **Right:** Close-up view of the BA.2.86 S-trimer interface of the RBD. The V445H substitution is represented by a stick model; arrows indicate the non-structural noise.

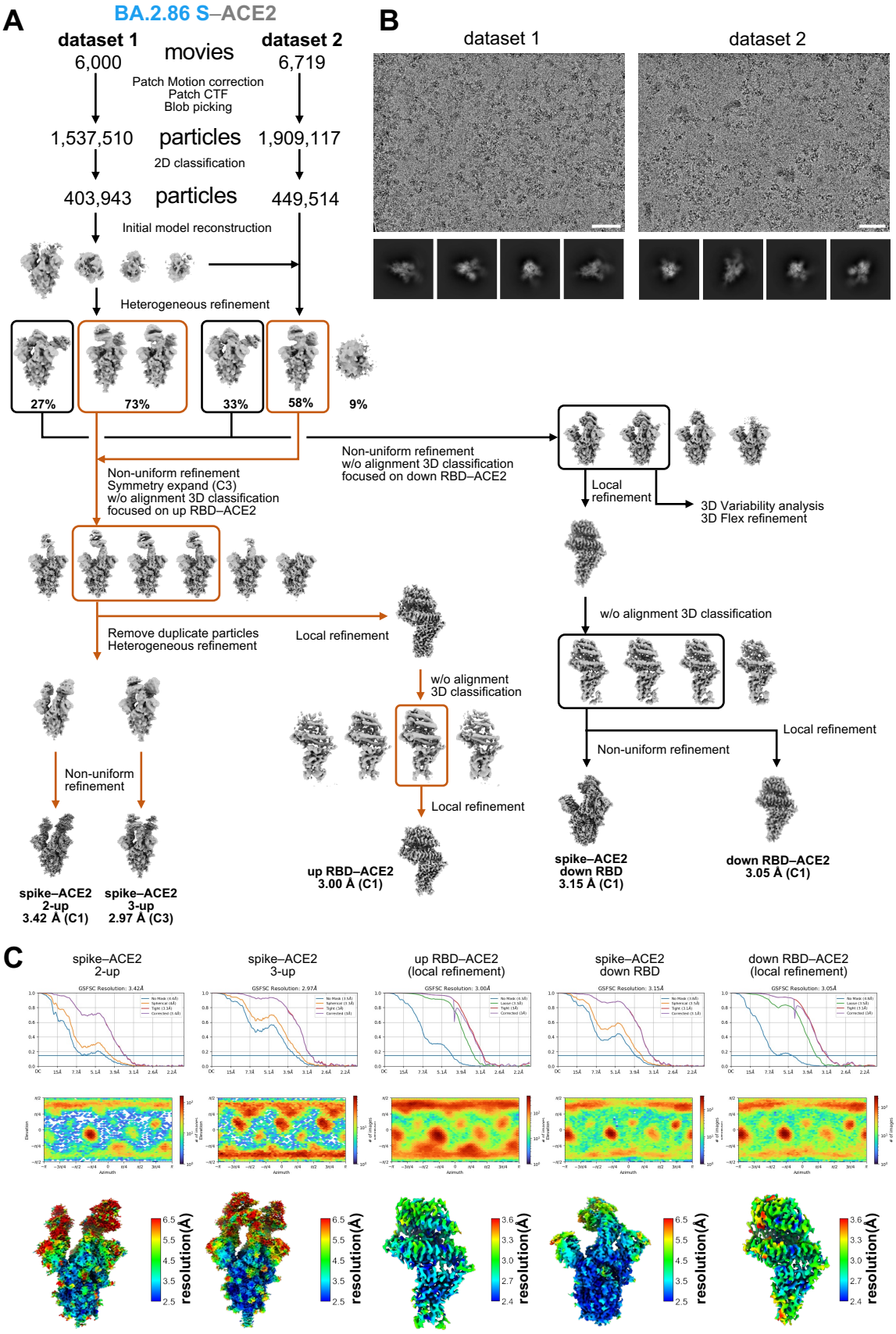

Supplementary Fig. 3. Workflow of cryo-EM data processing for BA.2.86 S–ACE2 complex
(A) Cryo-EM data-processing workflow for the SARS-CoV-2 BA.2.86 S–ACE2 complex. **(B) Top:** Representative micrographs (scale bars, 50 nm); **Bottom:** 2D class images. (C) **Top:** Global resolution assessment of cryo-EM maps using gold standard Fourier shell correlation (FSC) curves at 0.143 criteria. **Middle:** The angular distribution of particles representation by the viewing direction distribution plot. **Bottom:** The local resolution appears blue to red in each range.

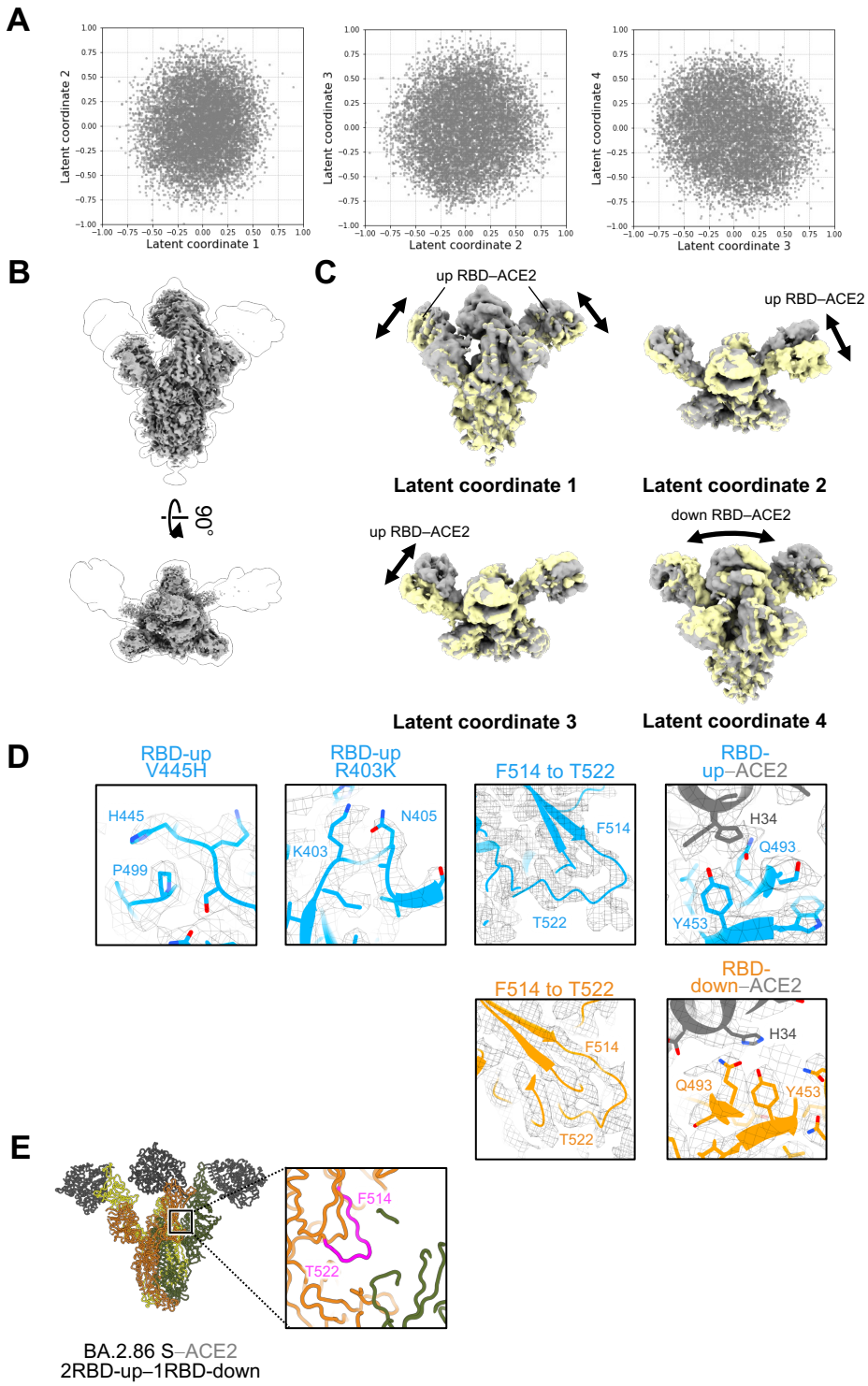

Supplementary Fig. 4. 3D Flexible on particle images of BA.2.86 S down-RBD bound to ACE2 state, and Cryo-EM maps of the RBD-ACE2 complex

(**A**) Scatter plots illustrating the dispersion of particle latent coordinates throughout the dataset of the BA.2.86 S two-up and one-down ACE2 complex. (**B**) Superimposition of cryo-EM maps for the BA.2.86 S two-RBD-up–one-RBD-down$_{\text{three ACE2}}$ and its 15 Å low-pass filtered maps. (**C**) Two representative cryo-EM maps for 3D Flexible refinement training along each of the four latent spaces: the first shows the mobility of two-up RBDs and ACE2; the second and third show the flexibility of one-up RBD and ACE2; the fourth shows all RBDs, including the down RBD–ACE2, as coordinately mobile. (**D**) Models fit to corresponding cryo-EM maps of specific residues shown in **Fig. 3B**. (**E**) The main-chain structure of the two-RBD-up–one-RBD-down$_{\text{three ACE2}}$ state (S, orange,yellow and dark olive green; ACE2, dark gray). In close-up views, the main chain from F514 to T522 appears magenta.

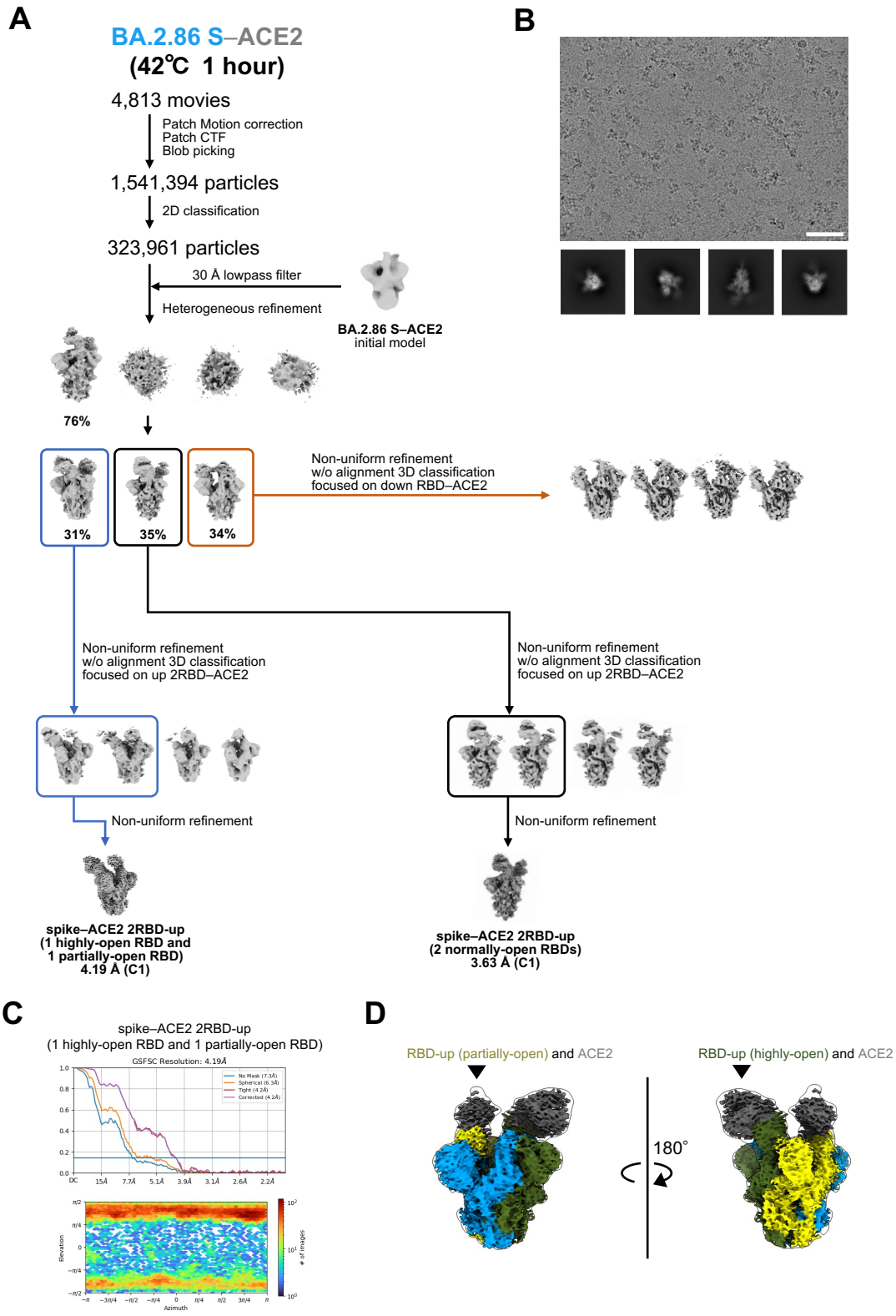

Supplementary Fig. 5. Workflow of cryo-EM data processing for BA.2.86 S–ACE2 complex treated at 42 ° C for 1 hour

(**A**) Cryo-EM data-processing workflow for the SARS-CoV-2 BA.2.86 S–ACE2 complex treated at 42 ° C for 1 hour. (**B**) **Top**: Representative micrographs (scale bars, 50 nm); **Bottom**: 2D class images. (**C**) **Top**: Global resolution assessment of cryo-EM maps using gold-standard Fourier shell correlation (FSC) curves at 0.143 criteria. The local resolution appears blue to red in each range. **Bottom**: The angular distribution of particles representation by the viewing direction distribution plot. (**D**) Cryo-EM map of BA.2.86 S–ACE2 non-canonical two-RBD-up (one-highly-open and one-partially-open; same colors as in **Fig. 2**).

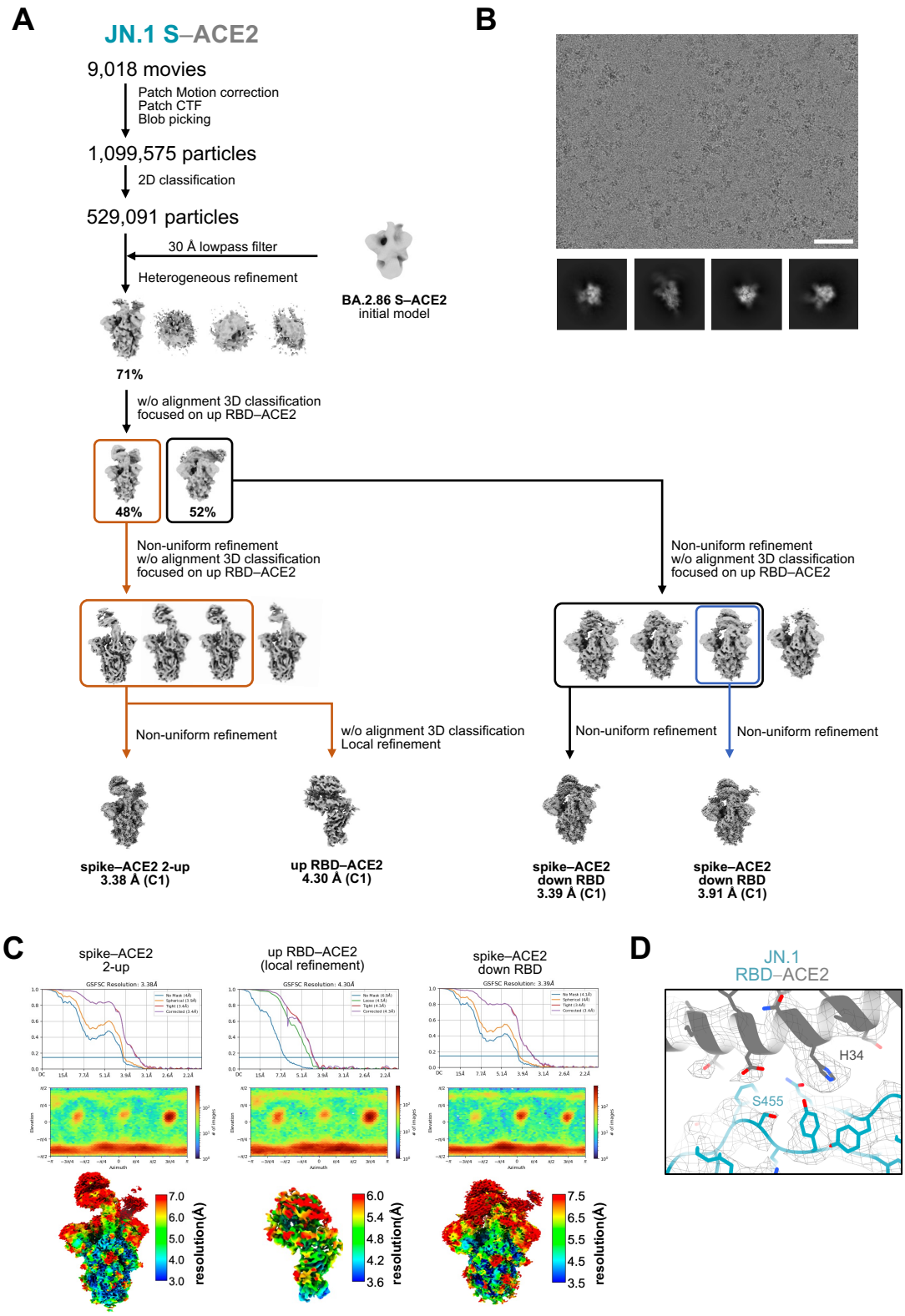

Supplementary Fig. 6. Workflow of cryo-EM data processing for JN.1 S–ACE2 complex
(**A**) Cryo-EM data-processing workflow for the SARS-CoV-2 JN.1 S–ACE2 complex. (**B**) **Top**: Representative micrographs (scale bars, 50 nm); **Bottom**: 2D class images. (**C**) **Top:** Global resolution assessment of cryo-EM maps using gold-standard Fourier shell correlation (FSC) curves at 0.143 criteria. **Middle:** The angular distribution of particles representation by the viewing direction distribution plot. **Bottom:** The local resolution appears blue to red in each range. (**D**) Models fit to corresponding cryo-EM maps of specific residues shown in **Fig. 3E**.

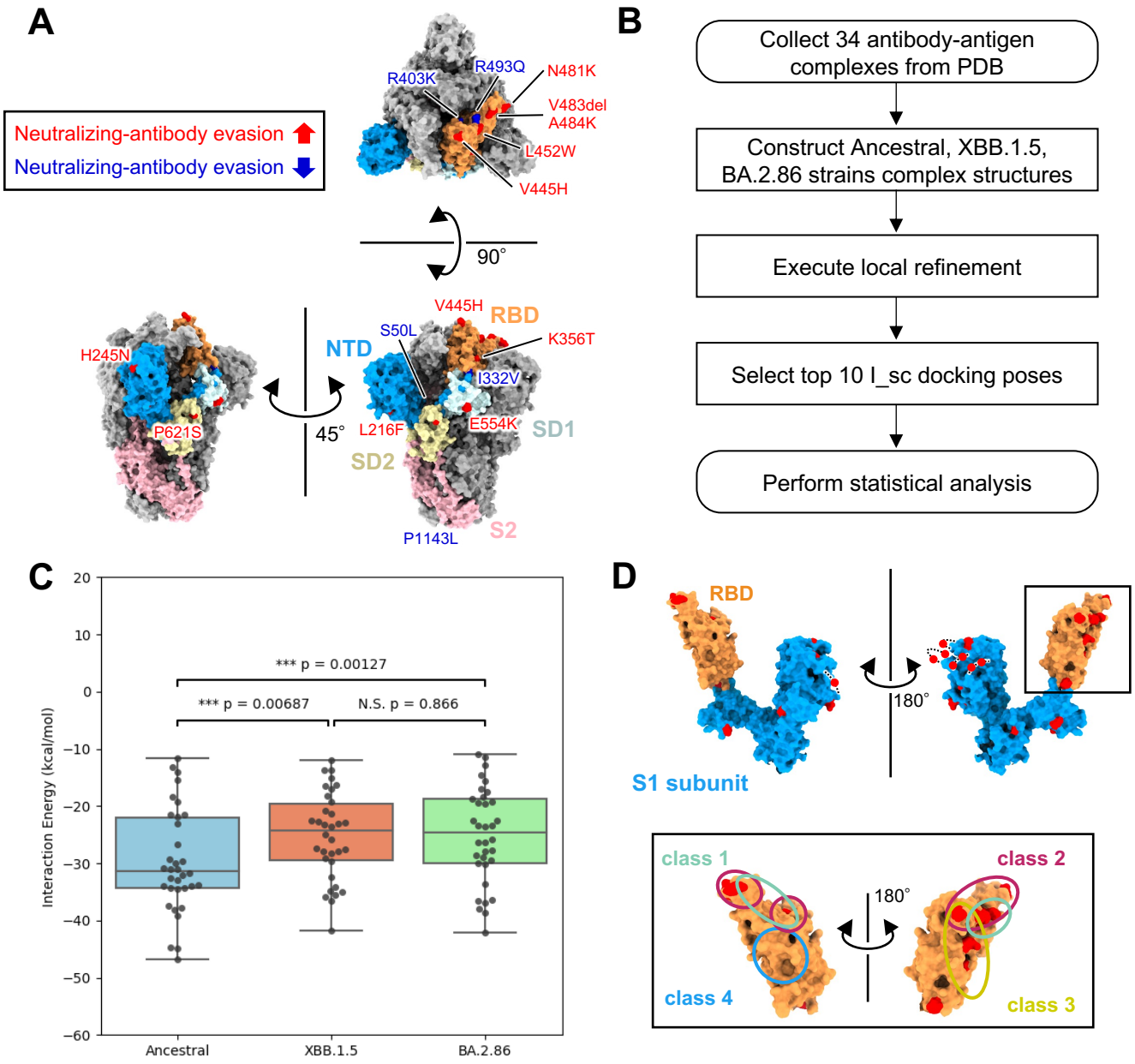

Supplementary Fig. 7. Potential for neutralizing-antibody evasion by amino-acid substitutions in the BA.2.86 S-protein

(**A**) Amino-acid substitutions associated with neutralizing-antibody evasion in the BA.2.86 S-protein (NTD; sky blue, RBD; orange, SD1; light blue, SD2; light yellow, S2; light pink). (**B**) Flowchart for computational evaluation of the neutralizing-antibody binding potential to S-proteins of ancestral strain, XBB.1.5, and BA.2.86. (**C**) Binding energy between S-proteins of ancestral strain, XBB.1.5, and BA.2.86 and 34 monoclonal antibodies that registered in the PDB. P-values were calculated using the Friedman test followed by a post-hoc Nemenyi test for group comparisons with Python 3.11.5 (***p < 0.001, **0.001<p < 0.01, *0.01 < p < 0.05). (**D**) Position of amino-acid substitutions in the BA.2.86 S1 subunit compared to that of XBB.1.5. Substitutions highlighted in red.

Supplementary Table 1. Cryo-EM data collection, refinement and validation statistics

	SARS-CoV-2 BA.2.86 spike		SARS-CoV-2 BA.2.86 spike-ACE2				
Data collection and processing	**closed**	**1-up**	**2-up**	**3-up**	**up-RBD ACE2 interface**	**2-up 1-down-ACE2**	**down-RBD ACE2 interface**
EMDB ID	EMD-37910	EMD-38459	EMD-38686	EMD-38690	EMD-38688	EMD-38687	EMD-38689
PDB ID	8WXL	8XUX	8XUY	8XVM	8XV0	8XUZ	8XV1
Microscope	Krios G4				Krios G4		
Camera	Gatan K3				Gatan K3		
energy filter	Gatan Biocontinuum				Gatan Biocontinuum		
slit width	20				20		
Magnification	130,000				130,000		
Recording mode	counting				counting		
Voltage (kV)	300				300		
Electron exposure (e–/Å^2)	52.45				51.39 or 51.16		
Exposure time (s)	1.5				1.5		
Number of raw frames	50				50		
Defocus range (μm)	-0.8 to -1.8				-0.8 to -1.8		
Pixel size (Å)	0.67				0.67		
Initial particle images (no.)	1,156,425				3,446,627		
Final particle images (no.)	91,823	32,669	36,340	41,431	215,827	829,61	829,61
Symmetry imposed	C3	C1	C1	C3	C1	C1	C1
Map resolution (Å)							
FSC 0.143	2.59	3.32	3.14	2.77	3.00	3.05	3.05
Refinement							
Initial model used (PDB code)	8IOT	8IOU	8IOU 8IOV	8IOU 8IOV	8IOU 8IOV	8IOV	8IOV
Model composition							
Protein residues	3120	3066	4266	4872	790	3306	794
Ligands	NAG:51	NAG:49	BMA:4 NAG:66, MAN:4	BMA:6 NAG:69, MAN:6	BMA:2 NAG:12, MAN:2	BMA:3 NAG:56, MAN:2	BMA:2 NAG:11, MAN:2
Map CC	0.87	0.86	0.83	0.83	0.82	0.84	0.81
R.m.s. deviations							
Bond lengths (Å)	0.004	0.003	0.004	0.003	0.002	0.002	0.002
Bond angles (°)	0.553	0.481	0.554	0.545	0.458	0.451	0.477
Validation							
MolProbity score	1.47	1.87	1.95	1.93	1.44	1.64	1.46
Clashscore	3.32	6.68	9.95	9.30	3.63	6.04	3.31
Rotamer outliers (%)	0.00	0.00	0.00	0.00	0.00	0.00	0.00
Ramachandran plot							
Favored (%)	94.93	91.58	93.32	93.16	95.80	95.58	95.19
Allowed (%)	5.07	8.42	6.68	6.84	4.20	4.42	4.81
Outliers (%)	0.00	0.00	0.00	0.00	0.00	0.00	0.00

(Supplementary Table 1, continued)

	SARS-CoV-2 BA.2.86 spike-ACE2 (treated at 42°C)	SARS-CoV-2 JN.1 spike-ACE2		
Data collection and processing	**2-up**	**2-up**	**2-up 1-down-ACE2**	**up-RBD ACE2 interface**
EMDB ID	EMD-60905	EMD-60904	EMD-60906	EMD-60886
PDB ID	-	-	-	9IU1
Microscope	Krios G4		Krios G4	
Camera	Gatan K3		Gatan K3	
energy filter	Gatan Biocontinuum		Gatan Biocontinuum	
slit width	20		20	
Magnification	130,000		130,000	
Recording mode	counting		counting	
Voltage (kV)	300		300	
Electron exposure (e–/Å^2)	50.985		51.233	
Exposure time (s)	1.5		1.5	
Number of raw frames	50		50	
Defocus range (μm)	-0.8 to -1.8		-0.8 to -1.8	
Pixel size (Å)	0.67		0.67	
Initial particle images (no.)	1,541,394		1,099,575	
Final particle images (no.)	37,922	151,272	173,979	149,071
Symmetry imposed	C1	C1	C1	C1
Map resolution (Å)				
FSC 0.143	4.19	3.39	3.63	4.30
Refinement				
Initial model used (PDB code)	-	-	-	8XV0
Model composition				
Protein residues	-	-	-	790
Ligands				BMA:2 NAG:12, MAN:2
Map CC	-	-	-	0.68
R.m.s. deviations				
Bond lengths (Å)	-	-	-	0.002
Bond angles (°)				0.512
Validation				
MolProbity score	-	-	-	2.00
Clashscore				9.20
Rotamer outliers (%)				0.00
Ramachandran plot				
Favored (%)	-	-	-	91.48
Allowed (%)				8.52
Outliers (%)				0.00

Supplementary Table 2. Binding energies of monoclonal antibodies to SARS-CoV-2 spike proteins

No.	Name1	Name2	PDB ID	PMID	Ave. I_sc	Ave. I_sc	Ave. I_sc
					Ancestral	XBB.1.5	BA.2.86
1	adg20	Adintenimab	7u2d	35487947	-29	-15	-16
2	adz8895	Tixagevimab	7l7d	34548634	-39	-28	-24
3	C144	Crexavibart	8dce	36103542	-32	-23	-23
4	COV2-2130	Cilgavimab	8d8q	36202799	-33	-19	-19
5	CT-P59	Regdanivimab	7cm4	33436577	-32	-25	-30
6	HB27	Upanovimab	7cyp	34676096	-19	-14	-11
7	J08	Simaravibart	7sbu	35549549	-38	-27	-28
8	LY-CoV016	Etesevimab	7c01	32454512	-34	-28	-26
9	LY-CoV1404	Bebtelovimab	7mmo	33972947	-33	-23	-23
10	LY-CoV555	Bamlanivimab	7kmg	33820835	-47	-26	-20
11	P2B-1G5	Romlusevimab	8gx9	-	-22	-21	-23
12	P2C-1F11	Amubarivimab	7cdi	33431856	-14	-34	-34
13	P4A1	Enuzovimab	7cjf	33976198	-45	-28	-30
14	REGN10933	Nepuvibart	6xdg	32540901	-23	-18	-18
15	REGN10987	Masavibart	6xdg	32540901	-18	-14	-15
16	S309	Sotrovimab	7jx3	32991844	-34	-35	-26
17	STE90-C11	Timcevibart	7b3o	34273271	-30	-28	-28
18	10-40	-	7sd5	35438546	-45	-42	-42
19	A19-46.1	-	7tca	35324257	-15	-16	-13
20	BD-515	-	7.00E+88	34021265	-31	-29	-26
21	BD55-4637	-	7wrj	36493787	-22	-23	-30
22	Beta-54	-	7ps6	34921776	-34	-21	-29
23	CoV2-2196	-	8d8r	36202799	-31	-24	-19
24	COVA1-16	-	7jmw	33242394	-34	-32	-36
25	CR3022	-	6w41	32245784	-34	-30	-29
26	H4	-	7l58	33794145	-21	-16	-17
27	Omi-18	-	7zfb	35662412	-31	-37	-37
28	Omi-3	-	7zf3	35662412	-34	-36	-39
29	Omi-42	-	7zr7	35662412	-12	-12	-11
30	SA55	-	7y0w	36493787	-37	-36	-38
31	SA58	-	7y0w	36493787	-38	-35	-37
32	XGv051	-	7wtf	35672388	-13	-17	-18
33	XGv347	-	7wea	35090164	-30	-23	-19
34	ZCB11	-	7xh8	35739114	-27	-23	-23

Supplementary Table 3. Details of human sera used in this study

SARS-CoV-2 infected	Donor ID	Sex	Age	Date of 1st vaccination (YYYY-MM-DD)	Date of 2nd vaccination (YYYY-MM-DD)	Date of 3rd vaccination (YYYY-MM-DD)	Date of 4th vaccination (YYYY-MM-DD)	Date of 5th vaccination (YYYY-MM-DD)	Date of 6th vaccination (YYYY-MM-DD)	Date of test (YYYY-MM-DD)	Date of sampling (YYYY-MM-DD)	Prior infection?
XBB.1.5	37071	Female	48	2021-10-01 (P)	2021-11-01 (P)	2022-05-06 (P)				2023-07-15	2023-08-11	No
XBB.1.5	36845	Male	29	2021-09-01 (M)	2021-09-29 (M)	2022-05-27 (M)				2023-06-26	2023-08-11	No
XBB.1.5	37229	Female	74	2021-06-24 (P)	2021-07-15 (P)	2022-02-16 (M)	2022-07-20 (M)	2023-03-25 (M)		2023-07-17	2023-08-01	No
XBB.1.5	36708	Male	55	2021-08-07 (P)	2021-08-27 (P)	2022-04-14 (P)				2023-06-01	2023-07-09	No
XBB.1.5	38084	Male	44	2021-09-13 (P)	2021-10-05 (P)	2022-07-29 (M)				2023-08-11	2023-09-02	No
XBB.1.5	37998	Female	65	2021-08-04 (P)	2021-08-30 (P)	2022-03-19 (M)	2022-09-02 (P)	2022-12-24(PBA.4/5)	2023-06-27 (P)	2023-08-10	2023-09-02	No
XBB.1.5	37798	Female	62	2021-03-17 (P)	2021-04-09 (P)	2021-12-23 (P)	2022-07-28 (P)	2023-06-17 (P)		2023-08-03	2023-08-20	No
XBB.1.5	38061	Female	55	2021-08-17 (P)	2021-09-18 (P)	2022-04-02 (M)	2022-10-14(PBA.1)			2023-08-11	2023-09-04	No
XBB.1.5	38019	Female	18	2021-09-07 (P)	2021-10-07 (P)	2022-04-28 (P)	2022-12-27 (P)			2023-08-10	2023-09-04	No
XBB.1.5	38952	Female	54	2021-07-27 (M)	2021-08-24 (M)	2022-03-24 (P)	2022-10-26 (P)			2023-08-23	2023-09-10	No

P, Pfizer-BioNTech; M, Moderna

Supplementary Table 4. Primers used in this study

Target region	Primer name	Primer sequence (5'-to-3')	Purpose
S protein	Omicron universal Fw	cactatagggcgaattgggtaccatgtttgtgttcctggt	Preparation of S expression plasmid
	BA.2 WT Rv	agctccaccgcggtggcggccgctcaggtgtagtgcagtttca	Preparation of S expression plasmid
	BA.2.86 K356 Fw	aggaagaggattagcaactgt	Preparation of S expression plasmid
	BA.2.86 K356 Rv	cctcttcctgttccaggcata	Preparation of S expression plasmid
	BA.2.86 V445 Fw	aaggtgagcggcaactacgac	Preparation of S expression plasmid
	BA.2.86 V445 Rv	gctcaccttgctgtccagctt	Preparation of S expression plasmid
	BA.2.86 P621 Fw	gtgcctgtggctatccatgct	Preparation of S expression plasmid
	BA.2.86 P621 Rv	cacaggcacctcagtacagtt	Preparation of S expression plasmid
	BA.2.86_N354Q Fw	tctgtctatgcctggcagaggaccaggattagc	Preparation of S expression plasmid
	BA.2.86_N354Q Rv	gctaatcctggtcctctgccaggcatagacaga	Preparation of S expression plasmid